Deglacial diatom production in the tropical North Atlantic driven by enhanced silicic acid supply

Katharine R Hendry[1], Xun Gong[2,3], Gregor Knorr[2,3], Jennifer Pike[2], & Ian R Hall[2]

[1]School of Earth Sciences, University of Bristol, Wills Memorial Building, Queen's Road, Bristol, BS8 1RJ, UK

[2]School of Earth and Ocean Sciences, Cardiff University, Main Building, Park Place, Cardiff, CF10 3AT, UK

[3]Alfred Wegener Institute, Bussestraße 24, D-27570 Bremerhaven, Germany

Abstract

Major shifts in ocean circulation are thought to be responsible for abrupt changes in temperature and atmospheric CO_2 during the last deglaciation, linked to variability in meridional heat transport and deep ocean carbon storage. There is also widespread evidence for shifts in biological production during these times of deglacial CO_2 rise, including enhanced diatom production in regions such as the tropical Atlantic. However, it remains unclear as to whether this diatom production was driven by enhanced wind-driven upwelling or density-driven vertical mixing, or by elevated thermocline concentrations of silicic acid supplied to the surface at a constant rate. Here, we demonstrate that silicic acid supply at depth in the NE Atlantic was enhanced during the abrupt climate events of the deglaciation. We use marine sediment archives to show that an increase in diatom production during abrupt climate shifts could only occur in regions of the NE Atlantic where the deep supply of silicic acid could reach the surface. The associated changes are indicative of enhanced regional wind-driven upwelling and/or weakened stratification due to circulation changes during phases of weakened Atlantic meridional overturning. Globally near-synchronous pulses of diatom production and enhanced thermocline concentrations of silicic acid suggest that widespread deglacial surface-driven breakdown of stratification, linked to changes in atmospheric circulation, had major consequences for biological productivity and carbon cycling.

Keywords: spicule, silicon isotope, Younger Dryas, Heinrich Stadial, upwelling

1. Introduction

Atmospheric CO_2 changes over the last glacial cycle have been associated with switches between different modes of Atlantic Meridional Overturning Circulation (AMOC): an interglacial mode with deep ventilation of North Atlantic Deep Water (NADW); a glacial mode with a shallower northern component (Glacial North Atlantic Intermediate Water, GNAIW); and a suppressed mode during Heinrich Stadials, most recently Heinrich Stadial One (HS1, 14.7-16.8 ka BP) and the Younger Dryas (YD, 11.5-12.8 ka BP), associated with iceberg rafting Heinrich Events during the last glacial termination (McManus et al., 2004). However, the change in AMOC between LGM and HS1 (Bradtmiller et al., 2014) and the exact nature of the link between ocean circulation and atmospheric CO_2 are still under debate (Böhm et al., 2015). Early Southern Hemisphere warming as a result of AMOC slow-down and reduced inter-hemispheric heat transport, amplified by Northern Hemisphere iceberg discharge, could shift the Southern Hemisphere westerly winds southwards, promoting widespread upwelling of CO_2-rich water and degassing of CO_2 into the atmosphere (Anderson et al., 2009). Alternatively, this early Southern Hemisphere warming could have led to shifts in oceanic circulation due to a reduction in GNAIW production resulting in changes in deep ocean density, ventilation and CO_2 release (Broecker, 1998; Meckler et al., 2013).

Silicic acid is an important nutrient for siliceous organisms such as diatoms and can be used as a water mass tracer in the modern Atlantic because there is a strong circulation driven south-north gradient in concentrations; Antarctic Bottom Water (AABW) is characterised by higher silicic acid concentrations than NADW (Fig. 1). Antarctic Intermediate Water (AAIW) and Subantarctic Mode Water (SAMW) are formed in the Southern Ocean by a combination of deep-water convection and wind-driven mixing near the Polar Front. The subducted intermediate depth water, which supplies a large area of the world's thermocline waters with nutrients, has moderate absolute concentrations of silicic acid, but low silicic acid concentration relative to other nutrients (e.g. nitrate) due to low nutrient utilisation by iron-limited diatoms (Sarmiento et al., 2004). Changes in the export of silicic acid, relative to other nutrients, in intermediate depth waters as a result of changes in iron supply to the Southern Ocean have been invoked as an explanation for glacial-interglacial pCO_2 changes (the Silicic Acid Leakage Hypothesis (Brzezinski et al., 2002)). However, there is arguably little evidence for either a change in the nutrient composition of AAIW or SAMW, or shifts in diatom growth relative to non-siliceous phytoplankton, over these timescales (Bradtmiller et al., 2006, 2007; Hendry and Brzezinski, 2014; Hendry et al., 2012).

61 The extent to which AAIW and SAMW distribution and nutrient composition changed during the
62 climatic events of the deglaciation is also far from clear. Nutrient proxies point towards an
63 increase in the export of nutrients from the Southern Ocean during HS1 and the YD (Came et al.,
64 2003; Hendry et al., 2012), but it is challenging to constrain their exact nature and source
65 (Meckler et al., 2013). Conservative tracers, such as the neodymium isotope composition of
66 ferromanganese coatings of detrital sediments and foraminifera, provide conflicting evidence
67 for either enhanced or reduced AAIW export into the tropical Atlantic during HS1 and the YD
68 (Huang et al., 2014; Pahnke et al., 2008; Xie et al., 2012). Comparable sediment archives from
69 the tropical Pacific show that there was an enhanced presence of AAIW and SAMW during the
70 same intervals (Pena et al., 2013).

71 Using a different approach, the flux of diatom opal and related geochemical
72 sedimentary properties (e.g. biogenic barium) have been used as a proxy for silicic acid supply,
73 to trace the route of deep southern component water (SCW) into the Atlantic (e.g. Meckler et
74 al., 2013). Pulses of diatom accumulation off the NW coast of Africa have been interpreted as
75 indicating that the Atlantic was filled with southern sourced glacial AABW (GAABW) during
76 glaciations. The boundary between northern and southern sourced waters shoaled further
77 during HS1 as a result of a strong AMOC reduction which allowed density-driven mixing
78 between surface waters and silicic acid-rich deep-waters (Meckler et al., 2013). However, the
79 driver of these pulses of diatom production remains unclear: were nutrients brought to the
80 surface at a greater rate as a result of stronger upwelling driven by stronger winds (Anderson et
81 al., 2009) or vertical mixing driven by density differences (Meckler et al., 2013)? Or did supply
82 rates stay relatively constant, with productivity enhanced by a greater concentration of the key
83 nutrient, silicic acid, feeding from below into the thermocline and eventually into the mixed
84 layer (Hendry et al., 2012)?

85 To understand the driver of pulses in diatom production we have reconstructed past
86 changes in deep-water silicic acid concentration in the mid- and high-latitude NE Atlantic using
87 the silicon isotope composition (denoted by δ^{30}Si) of siliceous sponge spicules (Hendry and
88 Robinson, 2012). The Iberian margin is ideally placed to investigate shifts in oceanographic
89 processes over millennial timescales due to high sedimentation rates and a strong sensitivity to
90 low and high latitude water exchange (Hodell et al., 2013). Furthermore, deep marine (>2500 m)

sediment cores have been found to record the balance of northern component water versus SCW in planktonic and benthic geochemical archives (Hodell et al., 2013).

2. Materials and Methods

2.1 Study sites

The site of sediment core OMEXII-9K (42°19.94'N, 09°41.92'W, 1833 m water depth; Hall and McCave, 2000) is bathed today in Upper Labrador Sea Water (40%), Upper Circumpolar Deep Water (20-30%) and Mediterranean Outflow Water (MOW, 30-40%) (Jenkins et al., 2015). We selected this location in order to investigate the vertical shift in the boundary between GNAIW and GAABW, which is thought to be at approximately 2000 m water depth at the latitude of the Iberian margin during the glacial (Gebbie, 2014). Although changes in MOW inflow could potentially change the bottom seawater chemistry at this location, MOW today has a low dissolved silicon concentration (Schlitzer, 2000) and there is no likely mechanism by which a change in composition of this water mass could cause any significant increase in silicic acid concentration at the core site. A northern-sourced end-member record from off the south east coast of Iceland (RAPiD-15-4P, 62° 17.58 'N, 17° 08.04 'W, 2133 m water depth) was selected as a comparison.

2.1. Silicon isotope measurements

Sponge spicules were hand-picked from the greater than 63 μm fraction of washed and sieved samples from sediment cores OMEXII-9K and RAPiD-15-4P and were cleaned according to published methods (Hendry and Robinson, 2012). Different spicule morphologies (megasclere types including different forms of, for example, triaenes, styles, tornotes) were monitored, to ensure that there were no biases introduced to the isotope measurements, and in order to give an indication of sponge diversity. The spicules were rinsed in deionized water, dried down in Teflon vials, then dried down again in 100 μL ultrapure concentrated HNO_3 (Romil) to remove any traces of organic matter. Whilst still hot, 500 μL of 0.4M NaOH (Merck Millipore TitriPUR) were added to each sample, and dissolved over three days at 100°C. The samples were acidified to pH~2 with 8N ultrapure HNO_3 (Romil), and purified using cation exchange resin (Bio-Rad AG50W X12) (Georg et al., 2006). Reference standards were prepared by alkaline fusion with NaOH pellets (Fisher Scientific), and processed as above (Georg et al., 2006).

The samples were analysed for silicon isotope composition (^{28}Si, ^{29}Si, ^{30}Si) using a Neptune Multi-Collector Inductively Coupled Plasma Mass Spectrometer (MC-ICP-MS) at Bristol University (operating conditions provided in Table S1). Machine blanks were monitored, and were <1% of the signal on ^{28}Si. A full procedural laboratory blank was processed and contained Si concentrations below the level of detection. Mass bias and matrix effects were corrected using standard-sample bracketing, and internal Mg-doping (Hendry and Robinson, 2012). Si and Mg intensities were matched within 10% (typically <5%). The silicon isotope results are reported as $\delta^{30}Si$ values relative to the standard NBS28 (SRM 8546) according to equation 1:

$$\delta^{30}Si = \left\{ \frac{\left(\frac{^{30}Si}{^{28}Si} \right)_{sample}}{\left(\frac{^{30}Si}{^{28}Si} \right)_{NBS28}} - 1 \right\} \times 1000 \quad (1)$$

Analysis of reference standards “diatomite” and “Big Batch”, which have been characterised by several research groups in an interlaboratory study, yielded a mean $\delta^{30}Si$ of -1.25 ‰ (±0.18 2SD, n = 70) and -10.67 ‰ (±0.08 2SD, n = 3) respectively, agreeing well with published values (Reynolds et al., 2007). Sponge standard LMG08 (Hendry et al., 2011; Hendry and Robinson, 2012) was analysed multiple times during every run and used to assess long-term external reproducibility, yielding mean $\delta^{29}Si$ and $\delta^{30}Si$ values over several months of -1.74 (±0.12) ‰ and -3.40 (±0.15) ‰ respectively (n = 37). Full sample replicates from OMEXII-9K agreed within 0.03‰. A three-isotope plot ($\delta^{29}Si$ vs. $\delta^{30}Si$) of all of the opal samples (including “diatomite”) measured in this study fall on a straight line through the origin with a gradient of 0.5106 ± 0.007 (1 SE), falling between thermodynamic (0.5210) and kinetic (0.5105) mass-dependent fractionation (Fig. 2). All isotope data are presented in the supplementary tables.

2.2. Silicic acid calculations

To account for the two published calibration models, silicic acid concentrations were calculated from spicule $\delta^{30}Si$ using the linear relationship from (Hendry et al., 2010; Hendry et al., 2012) for Southern Ocean sponges and the exponential relationship from (Hendry and Robinson, 2012; Wille et al., 2010) for sponges from different ocean basins including the Pacific. Seawater $\delta^{30}Si(OH)_4$ will influence the relationship between sponge $\delta^{30}Si$ and ambient silicic acid concentration (likely to be important for isotopically heavy waters e.g. AAIW). $\delta^{30}Si(OH)_4$ for the

South Atlantic site GeoB2017-3 (21.18°S, 46.45°W; 1048m water depth off the Brazilian margin) are from (Hendry et al., 2012). North Atlantic waters were assumed to have $\delta^{30}Si(OH)_4$ of +1.6‰ (de Souza et al., 2012).

2.3. Benthic foraminiferal calcite stable isotopes

To complement $\delta^{30}Si$ at OMEXII-9K, benthic foraminiferal (*Cibicidoides sp*.) calcite oxygen and carbon stable isotopes were measured from the deglacial section of the core (Supplementary tables). *Cibicidoides wuellerstorfi* and *C. pachyderma* were hand-picked from washed and sieved sediments from OMEXII-9K and measured for stable isotopes using a Thermo Finnigan MAT 252 isotope ratio mass spectrometer coupled to a Kiel II carbonate preparation device at Cardiff University.

2.4. Age Models

The age model for OMEXII-9K was based on radiocarbon measurements (from Hall and McCave, 2000) recalibrated using CALIB 7.1 and INTCAL13 with a reservoir age of 400 years; the percentage diatom data for the Iberian margin are from a nearby core MD95-2039 (40.57°N, 10.34°W, 3381 m water depth) with an age model based on reservoir-corrected radiocarbon measurements (from Vodelsang and Sarnthein, 2004) recalibrated using CALIB 7.1 and INTCAL13; other archives were dated using published age models using INTCAL04, 09 or 13 (Gherardi et al., 2005; Hendry et al., 2014; Hendry et al., 2012; McManus et al., 2004; Romero et al., 2008; Thornalley et al., 2011).

3. Results and discussion

3.1. NE Atlantic silicon isotopes and origins of deep water silicic acid

The $\delta^{30}Si$ measurements from RAPiD-15-4P range from -1.8 to -0.87‰, corresponding to silicic acid concentrations of <20 μM (Fig. 2d), with one value (dated as ~11.6 ka) of -2.06‰ corresponding to a higher silicic acid concentration (~30-40 μM). OMEXII-9K shows $\delta^{30}Si$ varying from -2.43 to -1.28‰ (silicic acid concentrations of <15-20 μM to ~50 μM), with a core top value of -1.51‰ that corresponds to a silicic acid concentration of ~20-25 μM, and matches well with modern observations from the Iberian margin (Fig.1, 3d). Downcore, OMEXII-9K has lower $\delta^{30}Si$ for the glacial compared to the Holocene, reflecting higher silicic acid concentrations. The deglaciation is punctuated by two very low $\delta^{30}Si$ peaks at 11.9-12.3 ka and 15.5-16.6 ka

(corresponding to peak silicic acid concentrations of 50-60 μM (Hendry et al., 2010; Hendry and Robinson, 2012)). There was no correspondence between spicule morphologies and isotopic composition, suggesting that there was no bias in the records resulting from spicule type or formation mechanism (supplementary tables and supplementary figure).

The relatively low silicic acid concentrations recorded by the SE Iceland RAPiD-15-4P core suggest that SCW did not penetrate into the high-latitude North Atlantic during HS1, and that our record from RAPiD-15-4P represents an area of NADW formation throughout the deglaciation. Persistent NADW formation is consistent with proxy reconstructions, including those based on $^{231}Pa/^{230}Th$ (Bradtmiller et al., 2014), εNd (Böhm et al., 2015) and grain size sortable silt (Hall and McCave, 2000), as well as model results (Gebbie, 2014), which suggest that the AMOC may only have weakened during HS1 and YD rather than collapsing entirely. The highest isotopic values, and so the lowest silicic acid concentrations, are recorded in RAPiD-15-4P at the beginning of the Bølling-Allerød (~ 14.7 ka), suggestive of either invigorated NADW production or a change in the source concentrations in the regions of deep water formation (Thornalley et al., 2011).

In contrast, the Iberian Margin OMEXII-9K core records abrupt shifts in silicic acid concentration towards high values during the deglacial, corresponding with the YD and HS1 and likely related to changes in Atlantic circulation. These low $\delta^{30}Si$ excursions in sponge values in our core closely correspond with Greenland ice core temperature fluctuations, although the Greenland signal is more pronounced in the YD compared to HS1 (Deplazes et al., 2013; Fig. 3a). The low isotope excursions also coincide, within age-model limits, with evidence from a nearby core for shifts in circulation strength according to $^{231}Pa/^{230}Th$ records (Fig. 3b; Gherardi et al., 2005), and occur at the same depths as negative excursions in benthic $\delta^{13}C$ recorded in OMEXII-9K (Fig. 3e). These contemporaneous excursions in benthic $\delta^{30}Si$ and $\delta^{13}C$, both towards lower values, are indicative of an incursion of nutrient-rich water onto the continental margin during periods of AMOC weakening. However, similar abrupt shifts towards higher silicic acid concentrations on the Iberian margin are not apparent in the OMEXII-9K record for either HS2 (~ 25 ka BP) or HS3 (~30 ka BP). While this could potentially be a consequence of lower sampling resolution during these intervals the lack of higher silicic acid concentrations is consistent with εNd records that point towards substantial weakening of AMOC only occurring during Heinrich Stadials at glacial terminations (Böhm et al., 2015). Between the HS1 and YD silicic acid

excursions, OMEXII-9K silicic acid returns to the northern component end-member values recorded in RAPiD-15-4P between 12.3 to 15.5 ka, consistent with reinvigorated AMOC and enhanced NADW formation during the Bølling-Allerød (Barker et al., 2010; Gherardi et al., 2005; McManus et al., 2004).

The lack of coincident shifts in spicule δ^{30}Si in our RAPiD-15-4P deglacial record off SE Iceland is a strong indication that the Iberian margin silicic acid pulses originated from the Southern Ocean. Using sponge spicule δ^{30}Si from Drake Passage, Southern Ocean and from RAPiD-15-4P as a measure of GAABW and GNAIW end-member silicic acid concentrations (assuming MOW to have a similar composition to GNAIW), we use mass balance to estimate that the water bathing the Iberian margin at our OMEXII-9K core site was ~50% GAABW during HS1 the YD (Fig. 4). Using modern end-member values for GAABW and GNAIW (plus MOW) of 120 and 15 μM respectively (Schlitzer, 2000) yields an estimate of ~70% GAABW contribution to the Iberian margin during HS1 and the YD. However, the silicic acid-rich pulses recorded by OMEXII-9K could have originated from either a greater extent of southern-sourced mode waters (GAAIW/SAMW) of relatively higher silicic acid concentration (Hendry et al., 2012; Pahnke et al., 2008), or through the entrainment of deep, silicic acid-rich waters into mode waters as a result of enhanced Southern Ocean ventilation (Anderson et al., 2009; Hendry and Brzezinski, 2014). Whilst it is not possible here to distinguish between these options, the evidence for changes in the extent of AAIW/SAMW during the deglaciation from foraminiferal stable isotopes and εNd records are equivocal, and only exist for the Western Atlantic (Huang et al., 2014; Pahnke et al., 2008; Xie et al., 2012) and Pacific (Crosta et al., 2007; Pena et al., 2013). It should also be noted that deglacial sponge spicule δ^{30}Si from the Brazilian margin (GeoB2107-3; Hendry et al., 2012), at 1000 m water depth, shows that AAIW/SAMW had sufficient silicic acid concentration to explain our Iberian margin record during the YD but are not sufficient to explain the high silicic acid peak during HS1 (Fig. 4). This may reflect an asymmetric zonal behaviour in the eastern and western Atlantic basins during the deglaciation, or different mechanisms controlling ocean circulation changes during the two abrupt events.

3.2. Origin of high silicic acid waters at the ocean surface

The close temporal link between the silicic acid incursions recorded in OMEXII-9K and diatom productivity archives from other regions of the mid-latitude NE Atlantic provides insight into the relative role of silicic acid supply, versus the concentration of thermocline waters, in the

development of deglacial opal peaks. Diatom abundance from sediment core GeoB7926 (20° 13'N, 18° 27'W, 2500 m water depth) off the NW coast of Africa (Romero et al., 2008), and other nearby locations (Meckler et al., 2013), show peaks during HS1 and the YD that are coeval with those from the OMEXII-9K spicule δ^{30}Si record (Fig. 5) that suggest a strong link between surface diatom production and deep water silicic acid concentrations. This similarity could be interpreted as supporting previous models that propose that the silicic acid reached the surface off NW Africa as a result of density-driven mixing between surface and deep ocean waters due to the reduction of the AMOC during HS1 (Meckler et al., 2013). However, importantly, diatom productivity records from the Iberian margin do not show any correspondence with our δ^{30}Si records of deep-water silicic acid concentration (Fig. 5). Such spatial variability and the localisation, in the NE Atlantic, of deglacial opal production to the NW coast of Africa indicates that there must have been an additional requirement met, as well as the presence of enhanced silicic acid concentration at depth, in order to promote diatom growth at these times.

The most likely additional key requirement necessary to drive enhanced diatom productivity is a regionally specific transport pathway of the silicic acid from depth to the surface ocean, promoted by, for example, localised wind-driven processes or density-driven stratification changes. In the modern ocean, the high surface productivity off the NW African coast is a result of the combined influence of nutrient supply and coastal upwelling (Romero et al., 2008). Relatively high-nutrient waters (up to 10μM silicic acid) reach the shelf as a result of sloping isopycnals (Boyer et al., 2013) and strong, near-coastal upwelling occurs continuously throughout the year driven by Ekman transport as a result of the trade winds (Huthnance, 1995). The upwelling is enhanced during the boreal winter when the Intertropical Convergence Zone (ITCZ) is in a southerly position and trade winds are strengthened (Adkins et al., 2006). Such high biomass waters that form within 50-70 km of the shore are additionally transported by surface currents in filaments that extend out to the open ocean (Pelegrí et al., 2005; Romero et al., 2008). A likely explanation for the increase in diatom production during the abrupt climate events of the deglaciation is that upwelling was strengthened relative to the Iberian margin as a result of enhanced trade winds, accompanying a southerly movement of the ITCZ, consistent with ^{230}Th and dust proxy and Th-normalised opal flux data (Adkins et al., 2006; McGee et al., 2014; Zhao et al., 2006), and coupled climate models (e.g. Chiang and Friedman, 2012). An increase in supply of upwelled waters to the near-shore coastal surface waters, together with an increase in nutrient concentration at depth and potentially stronger transport of high-biomass

filaments out to the open ocean, could readily explain the diatom abundances and species changes observed in GeoB7926 and greater export production from nearby cores (Filipsson et al., 2011; Incarbona et al., 2010; Moreno et al., 2002; Romero et al., 2008; Zarriess and Mackensen, 2010; Zhao et al., 2006). A wind-driven upwelling mechanism could also explain the lack of a significant diatom pulse at our Iberian margin site during HS1 and the YD, which is situated outside of the main trade wind belt. However, we cannot rule out that buoyancy driven changes in stratification, as a result of iceberg melt water inputs to the North Atlantic, led to latitudinal differences in the vertical density structure. Cold, fresh waters from the north could have led to greater stratification off the Iberian Margin, reducing nutrient supply to the surface and productivity (Incarbona et al., 2010), but could have contributed to weaken stratification and thus an enhanced upwelling of silicic acid into the surface waters in distal regions such as coastal NW Africa due to the warming in the subsurface depths of tropical Atlantic. Further modelling work will shed light on the relative roles of wind-driven and density-driven upwelling.

3.3. A global fingerprint of diatom production during the deglaciation

Comparison between our new δ^{30}Si isotope data and other paleoclimate records shows that the silicic acid-rich water reached intermediate depths only in certain regions of the Atlantic (Fig. 4). Sponge spicule δ^{30}Si records from a SW Atlantic core (GeoB2107-3, 1000 m water depth) show that AAIW was being exported from the Southern Ocean during HS1 and the YD with higher silicic acid concentrations (Hendry et al., 2012). Together with foraminiferal Cd/Ca records (Came et al., 2003), these published results indicate an increase in the ratio of silicic acid to other nutrients (nitrate and phosphate) during these abrupt climate events. This is consistent with enhanced ventilation in the Southern Ocean (Hendry and Brzezinski, 2014) potentially due to a Southern Ocean sea ice retreat that is accompanied by a southward shift of the sea ice melting zone and associated destratification (Abelmann et al., 2015). However, spicule δ^{30}Si records from a NW Atlantic core (KNR140-2-56GGC, 32° 56.3, 76° 17.7'W) from 1400 m water depth show marginally higher silicic acid concentrations during the glacial compared to the Holocene, and only a moderate increase in silicic acid during the deglaciation (Fig. 4) (Hendry et al., 2014). Although there is no evidence for any major increase in silicic acid at intermediate depths in the western basin of the North Atlantic (Fig. 4), there is evidence for increased diatom occurrence during the deglaciation in the western equatorial Atlantic (Bradtmiller et al., 2007)

and during HS1 in mid latitudes of the NW Atlantic (Hendry et al., 2014). Furthermore, equatorial Pacific biomarker (Calvo et al., 2011; Pena et al., 2013) and opal flux (Bradtmiller et al., 2006) records show periods of enhanced diatom production that are contemporaneous (within the limits of age models) with the deglacial Atlantic productivity peaks. Whilst these equatorial records appear – at least according to εNd records (Pena et al., 2013) - to coincide with peaks in GAAIW extent in the Pacific, the more complex pattern of intermediate water reconstructions in the Atlantic requires an explanation for the productivity peaks that does not rely on changes in mode water production or composition. Collectively these records require a mechanism to link biological activity in different ocean basins on rapid timescales, but which cannot solely be due to increased silicic acid concentrations from any one given source. We suggest an alternative explanation, in which widely-distributed regions of weakened stratification during HS1 and the YD, driven by atmospheric circulation changes, formed multiple conduits for nutrients and carbon to reach the ocean surface in several locations. These changes triggered particularly strong diatom production in those areas directly tapping into silicic acid-enriched deep SCW and thereby played a crucial role in deglacial changes in biological productivity and carbon cycling.

4. Conclusions

Major shifts in ocean circulation, driven by changes in the density structure and wind patterns, are thought to be responsible for the abrupt shifts in temperature and atmospheric CO_2 during the last deglaciation, as recorded in ice and marine sediment cores, due to links with heat transport between high and low latitudes, deep ocean carbon storage and biological productivity. This study presents the first evidence for an increase in the key nutrient silicic acid at depth, supplied to the North Atlantic during the abrupt climate events of the last deglaciation. This increase in silicic acid at depth would have driven the deglacial spikes of diatom growth observed in the Atlantic, in regions where physical processes would transport the deeper source of silicic acid towards the thermocline and the mixed layer. A global comparison of diatom growth proxies shows that these pulses of siliceous production occurred near-contemporaneously in regions of the Atlantic and Pacific, but were not ubiquitous. We suggest that there were widespread regions of weakened stratification during HS1 and the YD that triggered not only enhanced carbon release to the atmosphere, but also major changes in marine algal populations through changes in the supply of key nutrients.

Acknowledgments

The authors would like to thank I.N. McCave and D.J. Thornalley for samples and sample preparation; A. Clarke for benthic foraminifera analyses; C.D. Coath and A. Nederbragt for assistance with mass spectrometry. This study was funded by a NERC New Investigators Grant (NE/J00474X/1), a Royal Society University Research Fellowship, and A. Clarke was funded by a Cardiff Undergraduate Research Opportunities grant. Thank you to L.F Robinson and L. Bradtmiller, R.C. Xie, and two anonymous reviewers for their constructive comments.

References

Abelmann, A., Gersonde, R., Knorr, G., Zhang, X., Chapligin, B., Maier, E., Esper, O., Friedrichsen, H., Lohmann, G., Meyer, H., 2015. The seasonal sea-ice zone in the glacial Southern Ocean as a carbon sink. Nature communications 6.

Adkins, J., Demenocal, P., Eshel, G., 2006. The "African humid period" and the record of marine upwelling from excess 230Th in Ocean Drilling Program Hole 658C. Paleoceanography 21.

Andersen, K.K., Azuma, N., Barnola, J.-M., Bigler, M., Biscaye, P., Caillon, N., Chappellaz, J., Clausen, H.B., Dahl-Jensen, D., Fischer, H., 2004. High-resolution record of Northern Hemisphere climate extending into the last interglacial period. Nature 431, 147-151.

Anderson, R.F., Ali, S., Bradtmiller, L.I., Nielsen, S.H.H., Fleisher, M.Q., Anderson, B.E., Burckle, L.H., 2009. Wind-driven upwelling in the Southern Ocean and the deglacial rise in atmospheric CO2. Science 323, 1443-1448.

Barker, S., Knorr, G., Vautravers, M.J., Diz, P., Skinner, L.C., 2010. Extreme deepening of the Atlantic overturning circulation during deglaciation. Nature Geoscience 3, 567-571.

Böhm, E., Lippold, J., Gutjahr, M., Frank, M., Blaser, P., Antz, B., Fohlmeister, J., Frank, N., Andersen, M., Deininger, M., 2015. Strong and deep Atlantic meridional overturning circulation during the last glacial cycle. Nature 517, 73-76.

Boyer, T.P., Antonov, J.I., Baranova, O.K., Coleman, C., Garcia, H.E., Grodsky, A., Johnson, D.R., Locarnini, R.A., Mishonov, A.V., O'Brien, T.D., Paver, C.R., Reagen, J.R., Seidov, D., Smolyar, I.V., Zweng, M.M., 2013. World Ocean Database 2013, in: Levitus, S. (Ed.), NOAA Atlas NESDIS 72. Silver Spring, MD.

Bradtmiller, L.I., Anderson, R.F., Fleisher, M.Q., Burckle, L.H., 2006. Diatom productivity in the equatorial Pacific Ocean from the last glacial period to the present: a test of the silicic acid leakage hypothesis. Paleoceanography 21, doi: 10.1029/2006PA001282.

Bradtmiller, L.I., Anderson, R.F., Fleisher, M.Q., Burckle, L.H., 2007. Opal burial in the equatorial Atlantic Ocean over the last 30 ka: implicatons for glacial-interglacial changes in the ocean silicon cycle. Paleoceanography 22, doi:10.1029/2007PA001443.

Bradtmiller, L.I., McManus, J.F., Robinson, L.F., 2014. 231Pa/230Th evidence for a weakened but persistent Atlantic Meridional Overturning Circulation during Heinrich Stadial 1. Nature Communications 5.

Broecker, W.S., 1998. Paleocean circulation during the last deglaciation: a bipolar seesaw? Paleoceanography 13, 119-121.

Brzezinski, M.A., Sigman, D.M., Sarmiento, J.L., Matsumoto, K., Gruber, N., Rau, G.H., Coale, K.H., 2002. A switch from $Si(OH)_4$ to NO_3^- depletion in the glacial Southern Ocean. Geophysical Research Letters 29, 1564.

Calvo, E., Pelejero, C., Pena, L.D., Cacho, I., Logan, G.A., 2011. Eastern Equatorial Pacific productivity and related-CO2 changes since the last glacial period. Proceedings of the National Academy of Sciences of the USA 108, 5537-5541.

Came, R.E., Oppo, D.W., Curry, W.B., 2003. Atlantic ocean circulation during the Younger Dryas: insights from a new Cd/Ca record from the western subtropical South Atlantic. Paleoceanography 18, 1086, doi:1010.1029/2003PA000888.

Cardinal, D., Alleman, L.Y., de Jong, J., Ziegler, K., Andre, L., 2003. Isotopic composition of silicon measured by multicollector plasma source mass spectrometry in dry plasma mode. Journal of Analytical Atomic Spectrometry 18, 213-218.

Chiang, J.C., Friedman, A.R., 2012. Extratropical cooling, interhemispheric thermal gradients, and tropical climate change. Annual Review of Earth and Planetary Sciences 40, 383.

386 Crosta, X., Beucher, C., Pahnke, K., Brzezinski, M.A., 2007. Silicic acid leakge from the Southern
387 Ocean: opposing effects of nutrient uptake and oceanic circulation. Geophysical Research
388 Letters 34, L13601, doi:13610.13029/12006GL029083.
389 de Souza, G.F., Reynolds, B.C., Rickli, J., Frank, M., Saito, M.A., Gerringa, L.J.A., Bourdon, B.,
390 2012. Southern Ocean control of silicon stable isotope distribution in the deep Atlantic Ocean.
391 Global Biogeochemical Cycles 26, doi:10.1029/2011GB004141.
392 Deplazes, G., Lückge, A., Peterson, L.C., Timmermann, A., Hamann, Y., Hughen, K.A., Röhl, U., Laj,
393 C., Cane, M.A., Sigman, D.M., 2013. Links between tropical rainfall and North Atlantic climate
394 during the last glacial period. Nature Geoscience 6, 213-217.
395 Filipsson, H.L., Romero, O.E., Stuut, J.B.W., Donner, B., 2011. Relationships between primary
396 productivity and bottom-water oxygenation off northwest Africa during the last deglaciation.
397 Journal of Quaternary Science 26, 448-456.
398 Gebbie, G., 2014. How much did Glacial North Atlantic Water shoal? Paleoceanography 29, 190-
399 209.
400 Georg, R.B., Reynolds, B.C., Frank, M., Halliday, A.N., 2006. New sample preparation techniques
401 for the determination of Si isotopic composition using MC-ICPMS. Chemical Geology 235, 95-
402 104.
403 Gherardi, J.-M., Labeyrie, L., McManus, J.F., Francois, R., Skinner, L.C., Cortijo, E., 2005. Evidence
404 from the Northeastern Atlantic basin for variability in the rate of the meridional overturning
405 circulation through the last deglaciation. Earth and Planetary Science Letters 240, 710-723.
406 Hall, I.R., McCave, I.N., 2000. Palaeocurrent reconstruction, sediment and thorium focussing on
407 the Iberian margin over the last 140 ka. Earth and Planetary Science Letters 178, 151-164.
408 Hendry, K.R., Brzezinski, M.A., 2014. Using silicon isotopes to understand the role of the
409 Southern Ocean in modern and ancient biogeochemistry and climate Quaternary Science
410 Reviews 89, 13-26.
411 Hendry, K.R., Georg, R.B., Rickaby, R.E.M., Robinson, L.F., Halliday, A.N., 2010. Deep ocean
412 nutrients during the Last Glacial Maximum deduced from sponge silicon isotopic compositions.
413 Earth and Planetary Science Letters 292, 290-300.
414 Hendry, K.R., Leng, M.J., Robinson, L.F., Sloane, H.J., Blusztjan, J., Rickaby, R.E.M., Georg, R.B.,
415 Halliday, A.N., 2011. Silicon isotopes in Antarctic sponges: an interlaboratory comparison.
416 Antarctic Science 23, 34-42.
417 Hendry, K.R., Robinson, L.F., 2012. The relationship between silicon isotope fractionation in
418 sponges and silicic acid concentration: modern and core-top studies of biogenic opal.
419 Geochimica et Cosmochimica Acta 81, 1-12.
420 Hendry, K.R., Robinson, L.F., McManus, J.F., Hays, J.D., 2014. Silicon isotopes indicate enhanced
421 carbon export efficiency in the North Atlantic during deglaciation. Nature Communications 5.
422 Hendry, K.R., Robinson, L.F., Meredith, M.P., Mulitza, S., Chiessi, C.M., Arz, H., 2012. Abrupt
423 changes in high-latitude nutrient supply to the Atlantic during the last glacial cycle. Geology 40,
424 123-126.
425 Hodell, D., Crowhurst, S., Skinner, L., Tzedakis, P.C., Margari, V., Channell, J.E., Kamenov, G.,
426 Maclachlan, S., Rothwell, G., 2013. Response of Iberian Margin sediments to orbital and
427 suborbital forcing over the past 420 ka. Paleoceanography 28, 185-199.
428 Huang, K.-F., Oppo, D.W., Curry, W.B., 2014. Decreased influence of Antarctic intermediate
429 water in the tropical Atlantic during North Atlantic cold events. Earth and Planetary Science
430 Letters 389, 200-208.
431 Huthnance, J.M., 1995. Circulation, exchange and water masses at the ocean margin: the role of
432 physical processes at the shelf edge. Progress in Oceanography 35, 353-431.

433 Incarbona, A., Martrat, B., Di Stefano, E., Grimalt, J.O., Pelosi, N., Patti, B., Tranchida, G., 2010.
434 Primary productivity variability on the Atlantic Iberian Margin over the last 70,000 years:
435 Evidence from coccolithophores and fossil organic compounds. Paleoceanography 25.
436 Jenkins, W., Lott, D., Longworth, B., Curtice, J., Cahill, K., 2015. The distributions of helium
437 isotopes and tritium along the US GEOTRACES North Atlantic sections (GEOTRACES GAO3). Deep
438 Sea Research Part II: Topical Studies in Oceanography 116, 21-28.
439 Lippold, J., Grutzner, J., Winter, D., Lahaye, Y., Mangini, A., Christl, M., 2009. Does sedimentary
440 231Pa/230Th from the Bermuda Rise monitor past Atlantic Meridional Overturning Circulation?
441 Geophysical Research Letters 36, L12601, doi:12610.11029/12009GL038068.
442 McGee, D., Donohoe, A., Marshall, J., Ferreira, D., 2014. Changes in ITCZ location and cross-
443 equatorial heat transport at the Last Glacial Maximum, Heinrich Stadial 1, and the mid-
444 Holocene. Earth and Planetary Science Letters 390, 69-79.
445 McManus, J.F., Francois, R., Gherardi, J.-M., Keigwin, L.D., Brown-Leger, S., 2004. Collapse and
446 rapid resumption of Atlantic meridional circulation linked to deglacial climate changes. Nature
447 428, 834-837.
448 Meckler, A.N., Sigman, D.M., Gibson, K.A., Francois, R., Martinex-Garcia, A., Jaccard, S.L., Rohl,
449 U., Peterson, L.C., Tiedemann, R., Haug, G.H., 2013. Deglacial pulses of deep-ocean silicate into
450 the subtropical North Atlantic Ocean. Nature 495, 495-498.
451 Moreno, A., Nave, S., Kuhlmann, H., Canals, M., Targarona, J., Freudenthal, T., Abrantes, F.G.,
452 2002. Productivity response in the North Canary Basin to climate changes during the last
453 250,000 yr: a multi-proxy approach. Earth and Planetary Science Letters 196, 147-159.
454 Pahnke, K., Goldstein, S.L., Hemming, S.R., 2008. Abrupt changes in Antarctic Intermediate
455 Water circulation over the past 25,000 years. Nature Geoscience 1, 870-874.
456 Pelegrí, J., Arístegui, J., Cana, L., González-Dávila, M., Hernández-Guerra, A., Hernández-León, S.,
457 Marrero-Díaz, A., Montero, M., Sangrà, P., Santana-Casiano, M., 2005. Coupling between the
458 open ocean and the coastal upwelling region off northwest Africa: water recirculation and
459 offshore pumping of organic matter. Journal of Marine Systems 54, 3-37.
460 Pena, L., Goldstein, S.L., Hemming, S.R., Jones, K.M., Calvo, E., Pelejero, C., Cacho, I., 2013. Rapid
461 changes in meridional advection of Southern Ocean intermediate waters to the tropical Pacific
462 during the last 30 kyr. Earth and Planetary Science Letters 368, 20-32.
463 Reynolds, B.C., Aggarwal, J., Andre, L., Baxter, D., Beucher, C., Brzezinski, M.A., Engstrom, E.,
464 Georg, R.B., Land, M., Leng, M.J., Opfergelt, S., Rodushkin, I., Sloane, H.J., van der Boorn,
465 S.H.J.M., Vroon, P.Z., Cardinal, D., 2007. An inter-laboratory comparison of Si isotope reference
466 materials. Journal of Analytical Atomic Spectrometry 22, 561-568.
467 Romero, O.E., Kim, J.-H., Donner, B., 2008. Submillenial-to-millenial variability of diatom
468 production off Mauritania, NW Africa, during the last glacial cycle. Paleoceanography 23,
469 PA3218, doi:3210.1029/2008PA001601.
470 Sarmiento, J.L., Gruber, N., Brzezinski, M.A., Dunne, J.P., 2004. High-latitude controls of
471 thermocline nutrients and low latitude biological productivity. Nature 427, 56-60.
472 Schlitzer, R., 2000. Electronic atlas of WOCE hydrographic and tracer data now available. EOS
473 Trans. AUG 81, 45.
474 Thomson, J., Nixon, S., Summerhayes, C., Rohling, E., Schönfeld, J., Zahn, R., Grootes, P.,
475 Abrantes, F., Gaspar, L., Vaqueiro, S., 2000. Enhanced productivity on the Iberian margin during
476 glacial/interglacial transitions revealed by barium and diatoms. Journal of the Geological Society
477 157, 667-677.
478 Thornalley, D.J.R., Barker, S., Broecker, W.S., Elderfield, H., McCave, I.N., 2011. The deglacial
479 evolution of North Atlantic deep convection. Science 331, 202-205.

480 Vodelsang, E., Sarnthein, M., 2004. Age control of sediment core MD96-2039. PANGAEA
481 doi:10.1594/PANGAEA.143170.
482 Wille, M., Sutton, J., Ellwood, M.J., Sambridge, M., Maher, W., Eggins, S., Kelly, M., 2010. Silicon
483 isotopic fractionation in marine sponges: a new model for understanding silicon isotopic
484 fractionation in sponges. Earth and Planetary Science Letters,
485 doi:10.1016/j.epsl.2010.1001.1036.
486 Xie, R.C., Marcantonio, F., Schmidt, M.W., 2012. Deglacial variability of Antarctic Intermediate
487 Water penetration into the North Atlantic from authigenic neodymium isotope ratios.
488 Paleoceanography 27, doi:10.1029/2012/PA002337.
489 Zarriess, M., Mackensen, A., 2010. The tropical rainbelt and productivity changes off northwest
490 Africa: a 31,000-year high-resolution record. Marine Micropaleontology 76, 76-91.
491 Zhao, M., Mercer, J.L., Eglinton, G., Higginson, M.J., Huang, C.-Y., 2006. Comparative molecular
492 biomarker assessment of phytoplankton paleoproductivity for the last 160kyr off Cap Blanc, NW
493 Africa. Organic Geochemistry 37, 72-97.

494

495

Figure Captions:

Figure 1: Location of study sites and other cores discussed in the main text. Colour contours show silicic acid concentration at the 2000 m depth contour (Schlitzer, 2000), illustrating the low silicic acid concentrations in modern northern component waters compared to the silicic acid-rich southern component waters. Map produced using Ocean Data View.

Figure 2: Three isotope plot for opal silicon isotope data measured during this study (Bristol Isotope Group, Jan 2014-Feb 2015). See Table S1 for operating conditions. The linear regression was carried out using SigmaPlot 13.0.

Figure 3: Silicon isotope records from deep-sea sponge spicules from RAPiD-15-4P (SE Iceland) and OMEXII-9K (Iberian margin) compared with other climate records. a) Greenland NGRIP ice core oxygen isotope curve (Andersen et al., 2004); b) $^{231}Pa/^{230}Th$ record from the Iberian margin (Gherardi et al., 2005) (dark grey squares); $^{231}Pa/^{230}Th$ record from the Bermuda Rise (Lippold et al., 2009; McManus et al., 2004) (light grey squares, error bars show 2 standard error, SE); c) OMEXII-9K planktonic $\delta^{18}O$ record from G. bulloides *(Hall and McCave, 2000) (hollow triangles); d) sponge spicule $\delta^{30}Si$ from OMEXII-9K (solid black circles); sponge spicule record from RAPiD-15-4P (hollow grey circles, this study, vertical error bars show 2 standard deviations (SD); external reproducibility and horizontal error bars are estimates of uncertainties on age model; full replicates from OMEXII-9K agreed within 0.03‰; note reversed $\delta^{30}Si$ axes such that silicic acid increases up the page; e) benthic $\delta^{18}O$ record from* Cibicidoides *(solid diamonds, mixed* C. pachyderma *and* C. wuellerstorfi*, this study, error bars are 1 SD); benthic $\delta^{13}C$ record (hollow diamonds, this study). The light grey bars highlight abrupt climate events as recorded in North Atlantic ice cores.*

Figure 4: A comparison of a) spicule silicon isotope records (error bars show 2SD) and b) reconstructed silicic acid concentrations from the Atlantic. Records are from SE Iceland (RAPiD-15-4P, this study), NW Atlantic (KNR140-2056GGC (Hendry et al., 2014)), Iberian margin (OMEXII-9K, this study), the Brazilian margin in the South Atlantic (GeoB2107-3 (Hendry et al., 2012)), and the Southern Scotia Sea area of the Southern Ocean (PC034 in grey fill (Hendry et al., 2010)). Note that the spicule $\delta^{30}Si$-silicic acid calibration will be dependent on seawater $\delta^{30}Si(OH)_4$ (Hendry et al., 2012), which could be responsible for the heavier isotopic composition of spicules from the South Atlantic compared to the Iberian margin. The $\delta^{30}Si$ axis is reversed. Silicic acid concentrations were reconstructed using the calibrations in Methods (error bar in b shows estimated uncertainty on calibrations of ~15 μM (Hendry et al., 2012)). For core locations, see Figure 1.

Figure 5: Comparison of silicon isotope signal from the Iberian margin and NE Atlantic diatom abundance. a) sponge spicule $\delta^{30}Si$ from OMEXII-9K (solid circles; vertical error bars show 2 standard deviations (SD)); b) percentage of material comprising diatom valves from a sediment

core near to OMEXII-9K (MD95-2039 (Thomson et al., 2000)) (black diamonds); and c) diatom assemblages (valves/g) from sediment core GeoB7926 off the NW African Margin in the Mauritanian upwelling zone (Romero et al., 2008) (grey diamonds).

Figure 1

Click here to download high resolution image

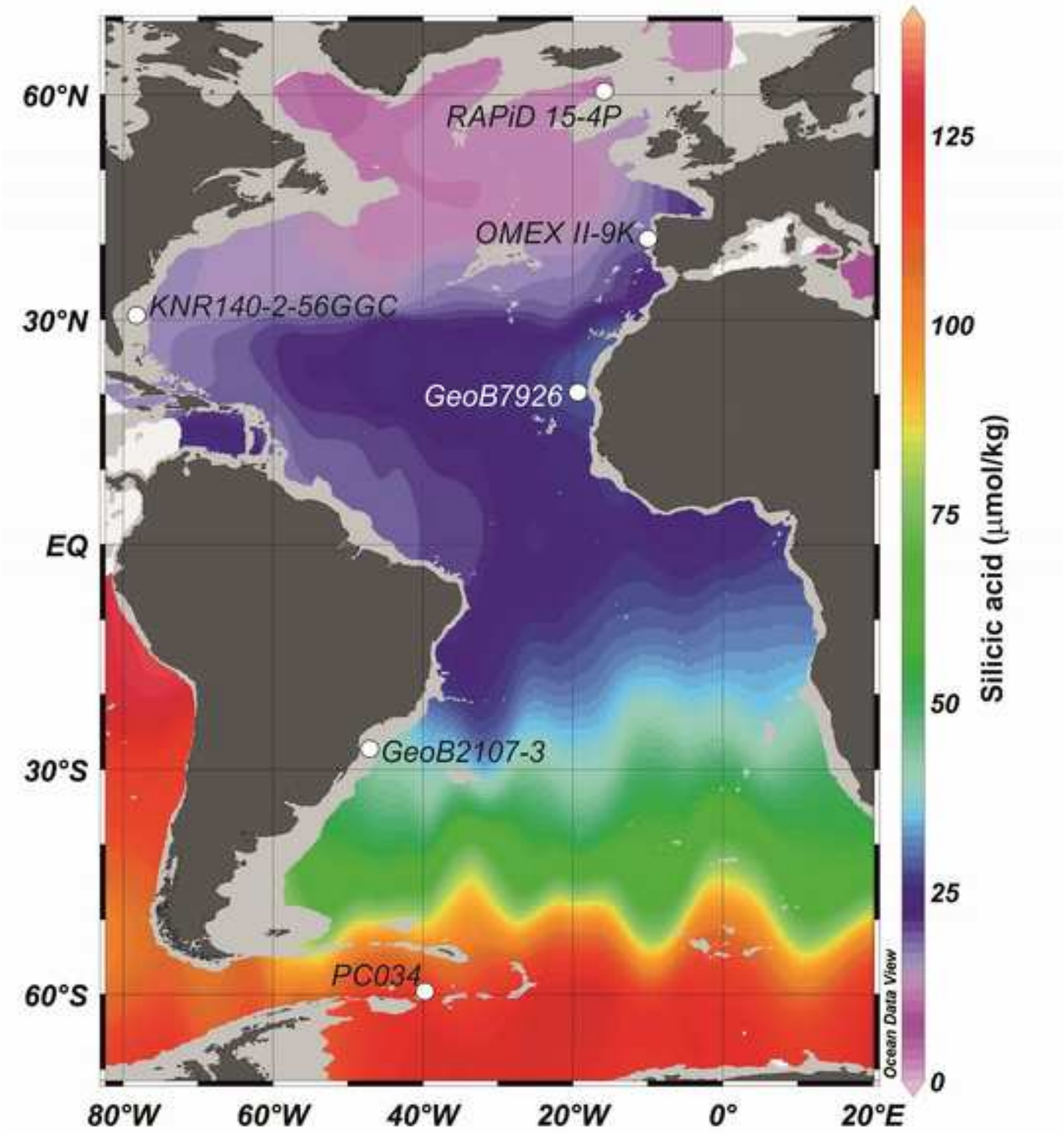

Figure 2
Click here to download high resolution image

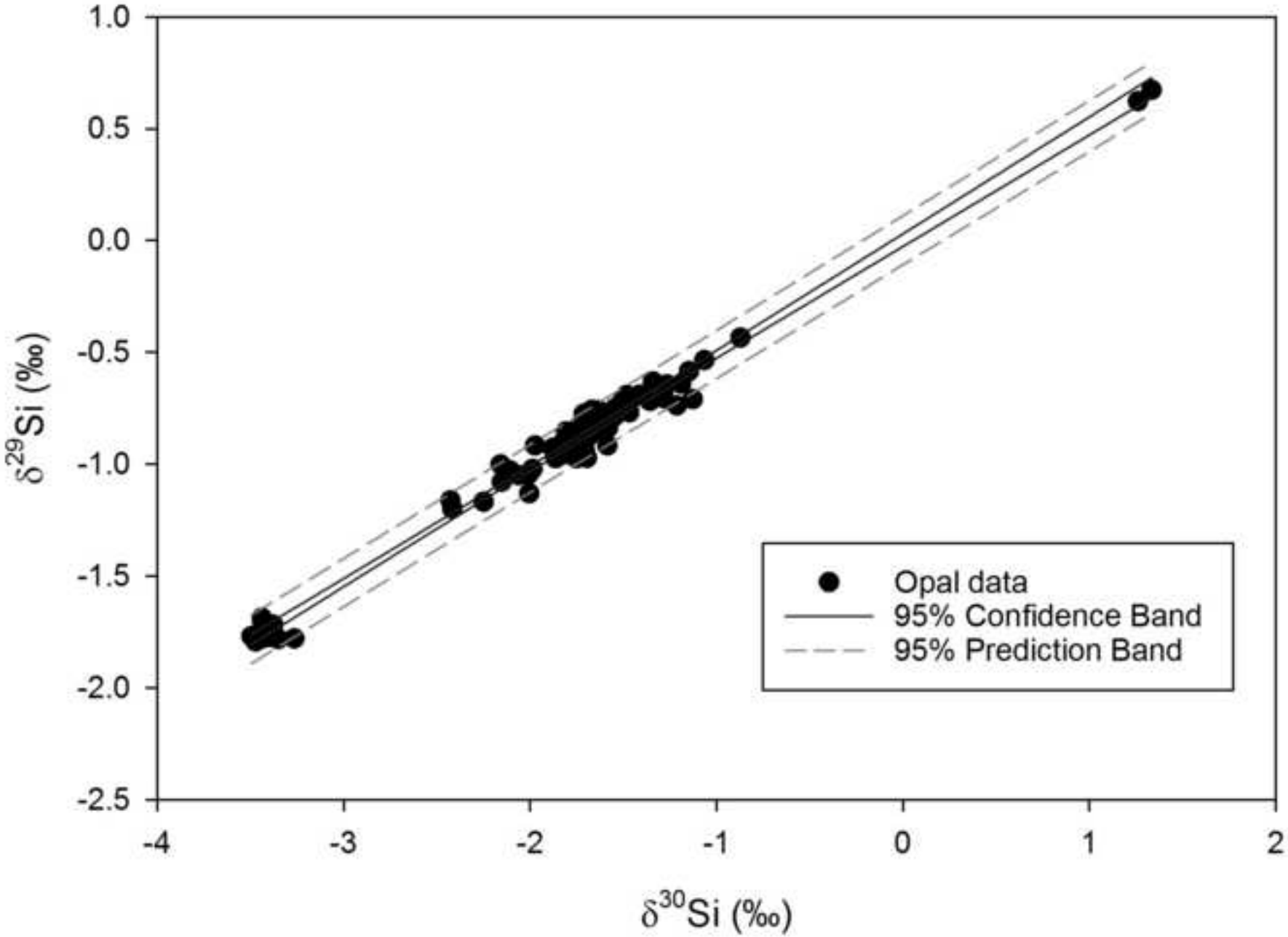

Figure 3

Click here to download high resolution image

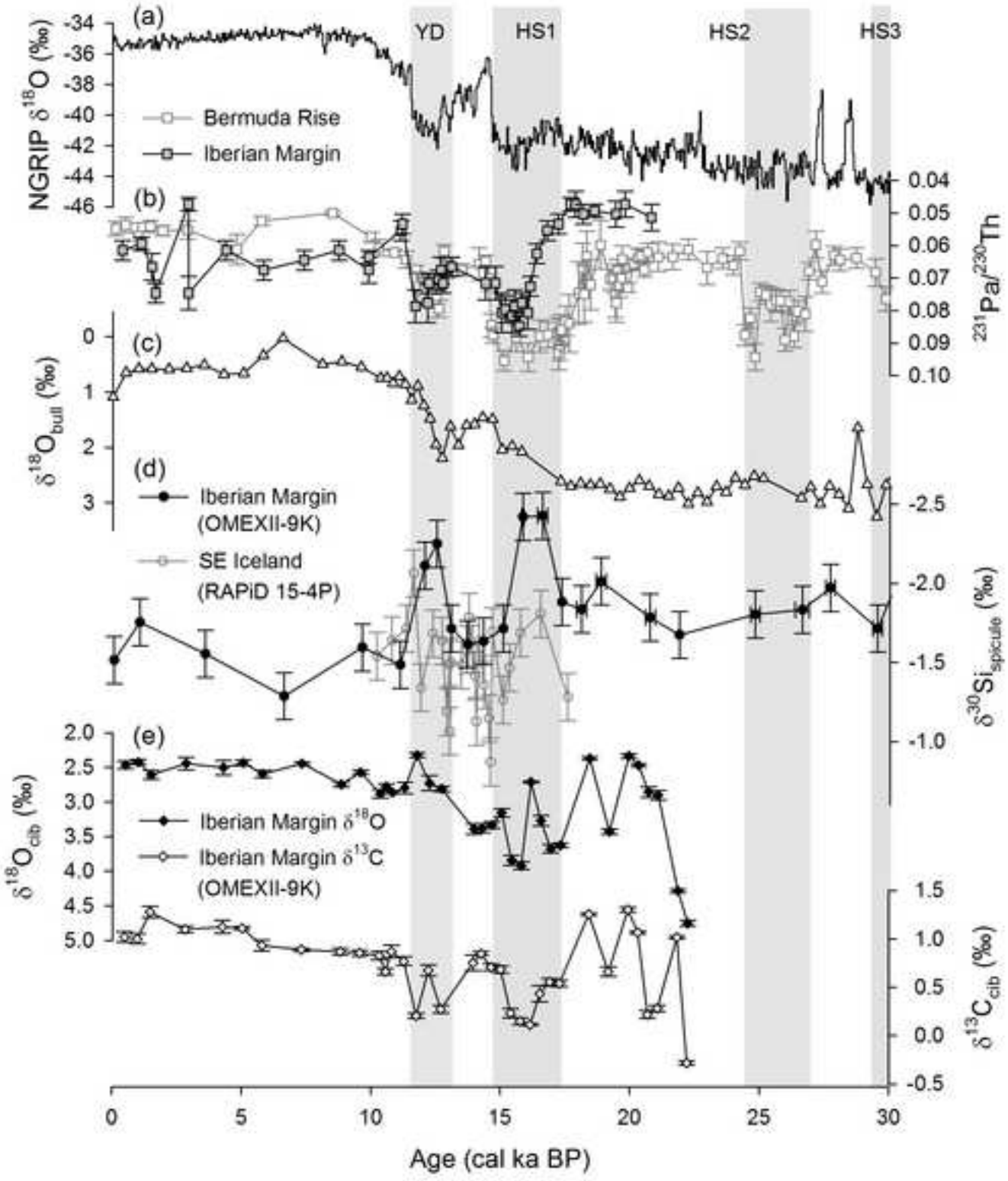

Figure 4a
Click here to download high resolution image

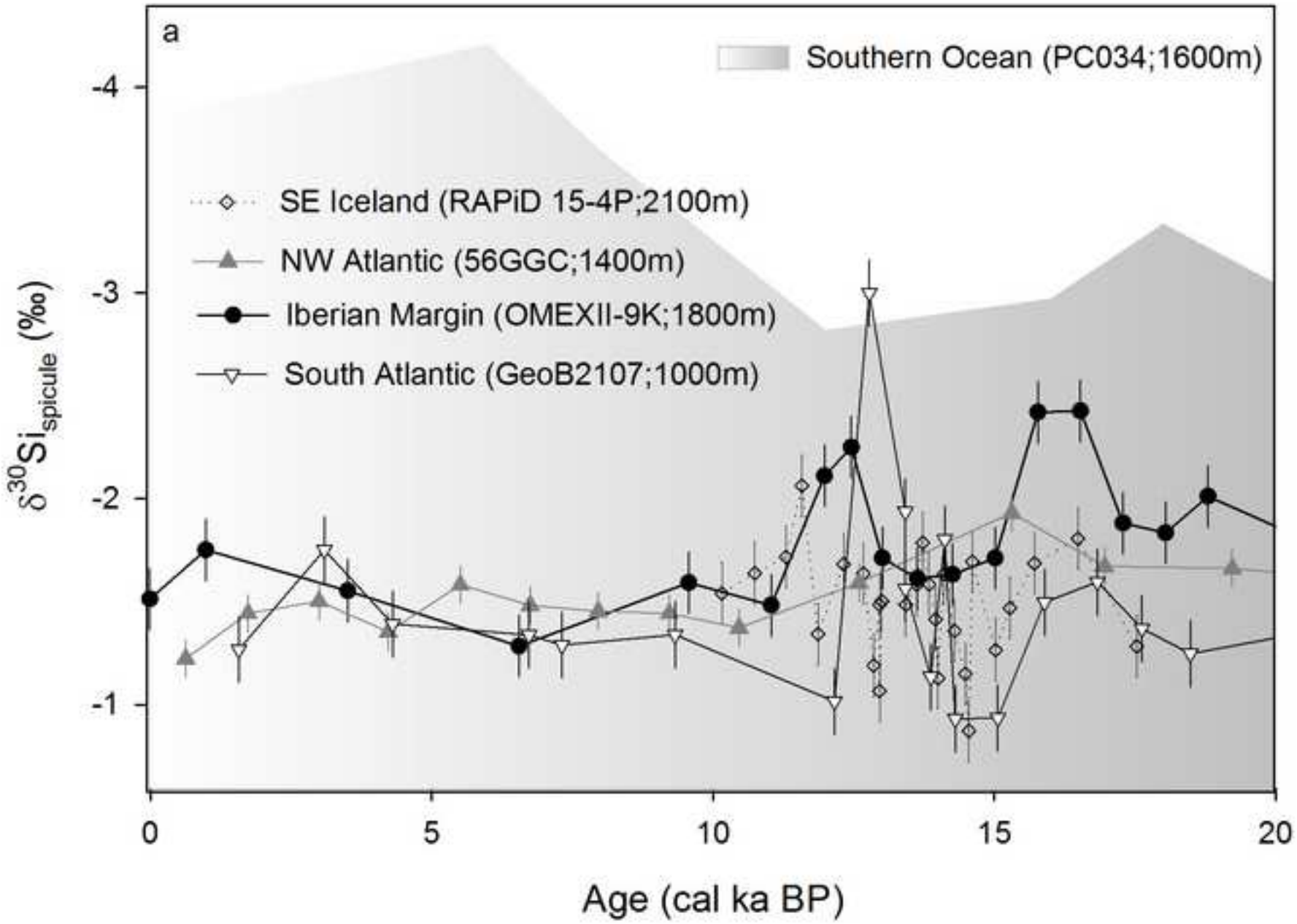

Figure 4b
Click here to download high resolution image

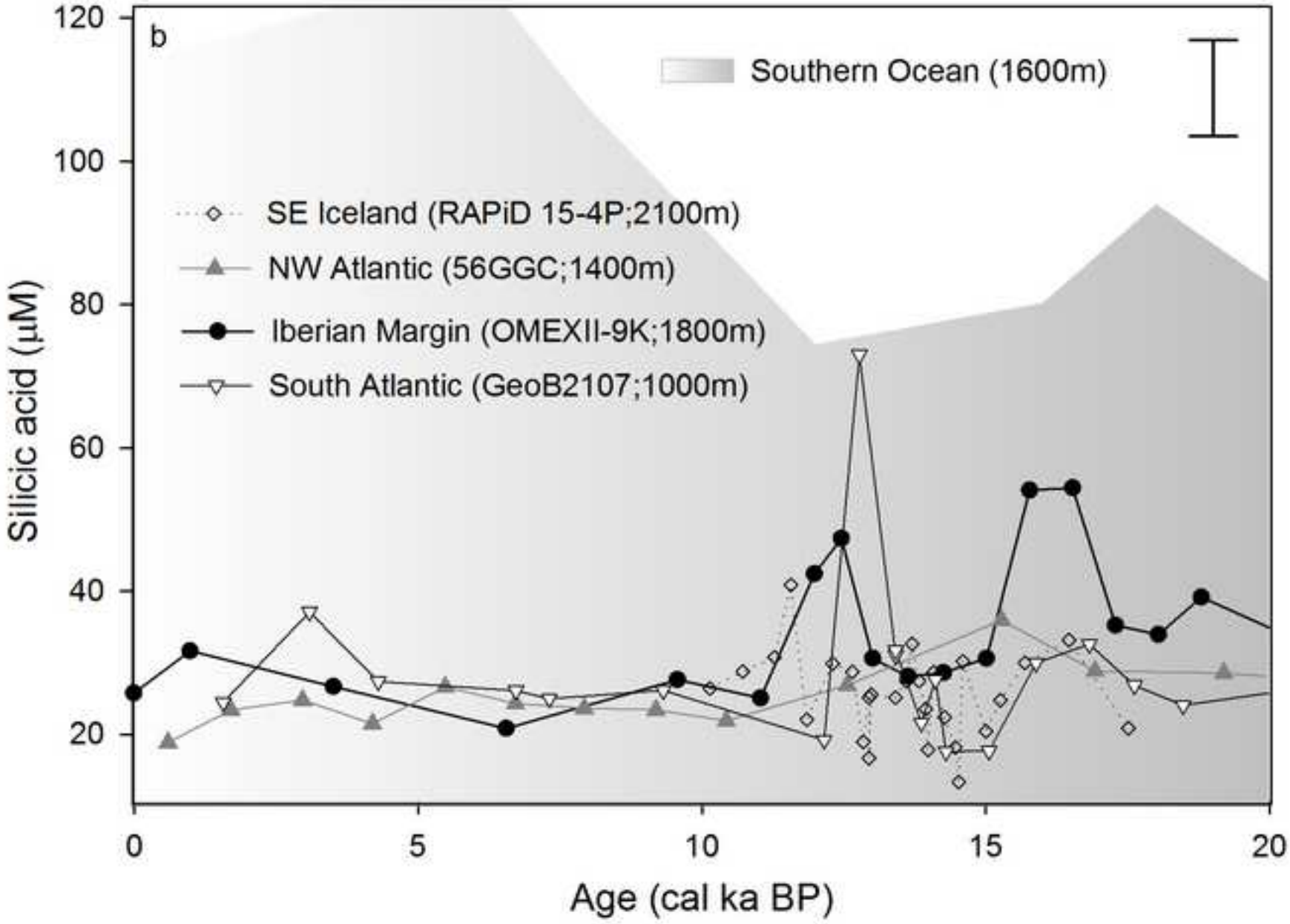

Figure 5

Click here to download high resolution image